Available online at www.sciencedirect.com
ScienceDirect
Polymer 48 (2007) 311–317
polymer
www.elsevier.com/locate/polymer

The effects of chemical structure on gas transport properties of poly(aryl ether ketone) random copolymers

M.L. Chng [a], Y. Xiao [a], T.S. Chung [a,*], M. Toriida [b], S. Tamai [b]

[a] *Department of Chemical and Biomolecular Engineering, National University of Singapore, 10 Kent Ridge Crescent, Singapore 119260, Singapore*
[b] *Material Science Laboratory, Mitsui Chemicals, Inc., 580-32 Nagaura Sodegaura-City, Chiba 299-0265, Japan*

Received 24 July 2006; received in revised form 31 October 2006; accepted 7 November 2006
Available online 28 November 2006

Abstract

The physical properties and gas permeation behavior of a series of homo/random copolymers of 4,4′-difluorobenzophenone (DFBP)–2,2-bis(4-hydroxy-phenyl)propane (BPA)/2,2-bis(4-hydroxy-3,5-dimethyl-phenyl)propane (TMBPA) have been investigated by systematically varying the diol ratios. The tetramethyl substitution group on the phenyl rings simultaneously increases polymer free volume and chain stiffness. These were confirmed by experimental and simulated methods. With the increase in TMBPA content, the gas permeation coefficients, diffusion and solubility coefficients of H_2, O_2, N_2, CO_2 and CH_4 were found to increase. The gas transport coefficients of the copolymers predicted from the additional rule were compared with the experimental results and the results obtained were within the expectations. In addition, the logarithm of gas permeation coefficients and the reciprocal of fractional free volume (1/FFV) also exhibited a good correlation. However, with the incorporation of TMBPA moiety, the permselectivity of gas pairs such as H_2/N_2, O_2/N_2 and CO_2/CH_4 remains reasonably high. As a result, the gas separation performance of TMBPA modified poly(aryl ether ketone) approaches the upper bound of the corresponding gas pairs. After comparing this work with gas separation performance of other methyl substituted polymers, one may conclude there is a general phenomenon that methyl substitution increases the gas permeability of the modified polymer with a small loss in gas selectivity for small gas pairs.

Keywords: Gas permeation; Poly(aryl ether ketone); Random copolymer

1. Introduction

Polymeric materials are utilized extensively for gas separation. Various membrane materials have been synthesized and investigated in the last two decades for their good gas separation and mechanical properties [1–3]. However, there still exists a tradeoff relationship between gas permeability and permselectivity for polymeric membranes [4,5]. To overcome the membranes' limitations, synthesizing new materials and modifying the existing membrane materials for better separation performance creates new market opportunities. It is now well documented that the gas permeability of polymeric materials can be improved by restricting the motion of polymer chains. Reducing the concentration of flexible linkages in the backbone, attaching bulky side groups, and cross-linking polymer chains have been widely studied to prepare new materials with high gas separation performance [6–8]. Among the above methods, attaching bulky side groups not only improve the gas diffusivity selectivity but also give a more open structure leading to higher gas permeabilities.

Synthesizing entirely new materials often involves high cost and lengthy period of time. In addition, the blending of different polymers also involves complicated phase behavior during membrane fabrication as most polymers are immiscible. Therefore copolymerization may be a more attractive option due to its simplicity, reproducibility, processibility and low development cost. Copolymerization of polymers is a simpler method which may synergistically combine the advantages of different material properties and eliminate the deficiencies of individual components [9–13].

* Corresponding author. Tel.: +65 6516 6645; fax: +65 6779 1936.
E-mail address: chencts@nus.edu.sg (T.S. Chung).

0032-3861/$ - see front matter © 2006 Elsevier Ltd. All rights reserved.
doi:10.1016/j.polymer.2006.11.009

Poly(aryl ether ketone), PAEK, is a glassy polymer widely used due to its high thermal stability, good mechanical properties and chemical resistance. Although a few studies have already shown the relationship between gas transport properties and the chemical structure of PAEK [14–16], improving PAEK gas separation performance by copolymerization is still not available. In order to have a more in-depth understanding of the relationship between the gas permeation behavior and the ratio of bulky side groups on the ether–ether phenyl ring, a series of homo/random copolymers PAEK from 4,4-difluorobenzophenone (DFBP), 2,2-bis(4-hydroxy-phenyl)propane (BPA), and 2,2-bis(4-hydroxy-3,5-dimethyl-phenyl)propane (TMBPA) in varying ratios were synthesized and their gas permeation properties were characterized. In addition, the previous works on the effects of methyl substitution on gas transport properties will also be reviewed and compared with this work.

2. Experimental

2.1. Materials

The PAEK copolymers used in this study were provided by Mitsui Chemical, Inc. 2,2-Bis(4-hydroxy-phenyl)propane (BPA), 2,2-bis(4-hydroxy-3,5-dimethyl-phenyl)propane (TMBPA), and 4,4′-difluorobenzophenone (DFBP) were used as received from Tokyo Kasei Kogyo Co. Ltd. Solvents and anhydrous potassium carbonate were obtained commercially and were used as received. The chemical structures of DFBP–BPA/TMBPA copolymers are shown in Fig. 1. Dichloromethane was employed as the solvent to prepare the dense membranes. Gases O_2, N_2, CH_4 and CO_2 with specified purities better than 99.9% were obtained from Soxal (except CH_4 from Linde).

2.1.1. Synthesis of PAEK copolymer (in case of BPA/TMBPA = 50/50)

A mixture of 11.3 g (0.0495 mol) of BPA, 14.1 g (0.0495 mol) of TMBPA, 21.8 g (0.1000 mol) of DFBP, and 17.1 g (0.1238 mol) of anhydrous potassium carbonate in 142 g of *N*-methyl-2-pyrrolidinone was stirred at 200 °C for 8 h under nitrogen atmosphere. It was then cooled down to 120 °C and poured into the mixture of methanol and water (1:1, 600 ml). The polymer was collected and first washed with 1500 ml of water, followed by washing with 1500 ml of methanol. The polymer was collected by filtration and dried at 180 °C for 4 h under nitrogen atmosphere. The yield was 39.5 g (92%). The inherent viscosity of the polymer was 0.64 dl/g, measured using an Ubbelohde viscometer in a solvent (NMP), at a concentration of 0.5 g/dl at 35 °C. The molecular weight distributions of the polymers were characterized using a Shodex GPC system-21H by means of a RI detector and a KF-803L*2 column with a flow rate of 1 ml/min. Tetrahydrofuran was used as the solvent and the testing temperature is maintained at 40 °C.

2.2. Preparation of dense membranes

A 2% (w/w) polymer solution was prepared by dissolving PAEK in dichloromethane (used as received). The polymer solution was then filtered through a Whatman filter (1 μm) to remove undissolved materials or dust particles and cast onto a stainless steel ring mounted on a leveled silicon wafer at ambient temperature. The casting ring was covered with a piece of glass and a small gap was kept for slow solvent evaporation. After slow solvent evaporation for about four days, the membrane was dried at 60 °C in a vacuum oven for one day to remove the residual solvent. The membrane was then heated at a rate of 12 °C/20 min to 20 °C above the T_g of the polymer and hold for 20 min before air quenching to room temperature. After the drying procedure, all membranes were cut into circles of 38 mm diameter and their thicknesses were measured by a Mitutoyo digital micrometer with a resolution of 1 μm. Only the membranes with about 60 ± 5 μm thickness were used in the following studies.

2.3. Physical properties characterization

The thermal stability of the dense films was evaluated using Shimadzu 50 type thermogravimetric analyser (TGA) to analyse their thermal stability. Under air atmosphere, the polymers were heated at a rate of 10 °C/min. All the PAEKs exhibit good thermal stability and the 5% decomposition temperatures were above 400 °C. The glass transition temperatures were

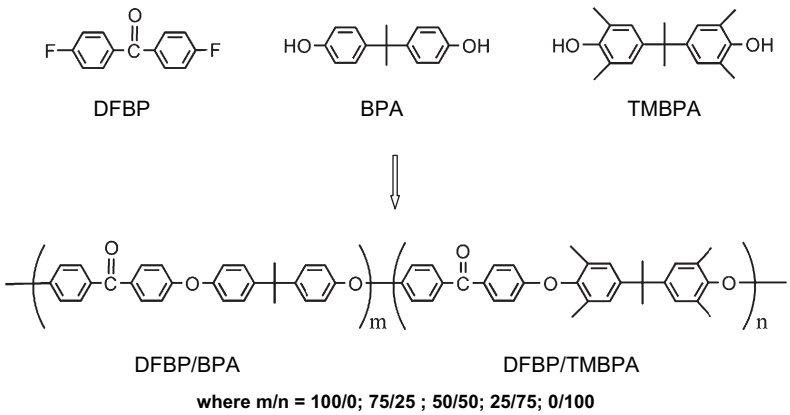

Fig. 1. Chemical structure of DFBP–BPA/TMBPA copolymers.

determined using Shimadzu 60 type differential scanning calorimeter (DSC) with a heating rate of 10 °C/min under nitrogen purge.

Densities of the PAEK dense films were measured at room temperature using an electronic Mettler Toledo balance with a density kit according to the Archimedean principle by recording the weight of the sample in air and ethanol. The density was calculated as follow:

$$\rho_{\text{polymer}} = \frac{w_{\text{air}}}{w_{\text{air}} - w_{\text{ethanol}}}\rho_{\text{ethanol}} \quad (1)$$

where w_{air} and w_{ethanol} are the film weights in air and in high purity ethanol (99.9%), respectively.

Wide-angle X-ray diffraction (WAXD) was performed using a Brukel X-ray diffractometer at room temperature with Cu Kα radiation wavelength of 1.54 Å. *d*-Spacing can be calculated from Bragg's rule as follows: $n\lambda = 2d\sin\theta$, where d is the dimension spacing, θ is the diffraction angle, λ is the X-ray wavelength and n is an integral number (1, 2, 3…).

A RMMC (the "RIS" Metropolis Monte Carlo method) module within the Cerius2 software package was used to calculate the properties of polymer chains, such as the mean squared end-to-end distance, mean squared radius of gyration, persistence length and molar stiffness function of the monomers and polymer chains.

2.4. Gas transport properties estimation

Two approaches were used to estimate the permeability coefficients of the copolyimides namely the addition rule and FFV [17] as shown in Eqs. (2) and (3), respectively.

$$\ln P = \phi_1 \ln P_1 + \phi_2 \ln P_2 \quad (2)$$

$$\ln P = A - \frac{B}{\text{FFV}} \quad (3)$$

where P is the permeability coefficient, ϕ is the volume fraction and subscripts 1 and 2 refer to the two homopolymers. A and B are adjustable characteristics parameters which depend solely on the nature of the penetrant/polymer system.

2.5. Gas permeation measurement

The pure gas permeability coefficients were measured by using a constant volume method. The testing temperature is maintained at 35 °C and the feed pressure is 10 atm for all the gases except H_2 which is tested at a lower pressure of 3.5 atm. Gases were measured in the sequence H_2, O_2, N_2, CH_4 and CO_2 and each data point is the average of three experimental data. Detailed experimental procedure and apparatus design could be found in the publication elsewhere [12]. In the present work, no polymers studied showed sign of plasticizations when exposed to CO_2 from 10 atm to 50 atm.

From the slope of the pressure curve on the permeation side vs. time, pure gas permeability coefficient can be calculated at a steady state using the following equation:

$$P = \frac{273\times10^{10}}{760}\frac{VL}{AT\left(\frac{p_2\times76}{14.7}\right)}\left(\frac{\mathrm{d}p}{\mathrm{d}t}\right) \quad (4)$$

where P is the permeability coefficient of the membrane to gas i (1 barrer $= 1\times10^{-10}$ cm^3 (STP) cm/cm^2 s cmHg), V is the downstream volume (cm^3), L is the thickness of the membrane (cm), A is the effective area of the membrane (cm^2), T is the absolute temperature (K), P_2 is the upstream pressure of the penetrant gas (psia) and dp/dt is the rate of pressure increase in the low-pressure downstream chamber (mmHg/s).

The apparent diffusion coefficients were predicted from the time lag method, the time taken to reach steady state, by the following relationship:

$$D_{\text{app}} = \frac{L^2}{6t} \quad (5)$$

where L is the film thickness (cm) and t is the time lag (s).

Apparent solubility coefficient S_{app} (cm^3 (STP)/cm^3 cmHg) may be calculated from the ratio of permeability coefficient to diffusion coefficient relationship:

$$S_{\text{app}} = \frac{P}{D_{\text{app}}} \quad (6)$$

Ideal permselectivity of a membrane for gas A to gas B for permeability, diffusivity and solubility were calculated as follows:

$$\alpha^P_{\text{A/B}} = \frac{P_{\text{A}}}{P_{\text{B}}} \quad (7)$$

$$\alpha^D_{\text{A/B}} = \frac{D_{\text{A}}}{D_{\text{B}}} \quad (8)$$

$$\alpha^S_{\text{A/B}} = \frac{S_{\text{A}}}{S_{\text{B}}} \quad (9)$$

3. Results and discussion

3.1. Thermal and physical properties

The thermal and physical properties of homo and various DFBP–BPA/TMBPA random copolymers studied in this work are listed in Table 1. The degradation temperatures (which are defined as the temperature where 5 wt% loss is achieved) of these PAEK polymers are in the range of 436–511 °C. The degradation temperature decreases with increasing TMBPA fraction in the polymer backbone, indicating that the methyl groups on the phenyl rings in TMBPA units are not thermally stable.

It can be seen that the glass transition temperature of DFBP–TMBPA is higher than that of DFBP–BPA. Compared with the structure of DFBP–BPA, DFBP–TMBPA copolyimides have four methyl substitutions on the phenyl ring, which disrupt the chain packing and hinder the phenyl ring rotation and thus result in an increase in rigidity of the backbone. The DSC curves for the random DFBP–BPA/TMBPA

Table 1
Physical properties of DFBP–BPA/TMBPA copolymers

Polymer ID	T_g (°C)	T_d (°C)	d (g/cm^3)	V (cm^3/g)	V_o (cm^3/mol; cm^3/g)	V_f (cm^3/g)	$V_{f,mix}$ (cm^3/g)	FFV
DFBP–BPA	153	511	1.186	0.843	294.6; 0.726	0.117	0.117	0.139
DFBP–(BPA75 + TMBPA25)	171	480	1.161	0.861	309.1; 0.736	0.125	0.124	0.145
DFBP–(BPA50 + TMBPA50)	188	458	1.143	0.875	323.6; 0.746	0.129	0.131	0.148
DFBP–(BPA25 + TMBPA75)	201	447	1.121	0.892	338.1; 0.755	0.137	0.138	0.154
DFBP–TMBPA	217	436	1.103	0.907	352.6; 0.763	0.144	0.144	0.159

copolymers showed a single T_g between that of the two homopolymers. The glass transition temperatures of random copolymers are estimated by the Fox equation [18]:

$$\frac{1}{T_g} = \frac{W_1}{T_{g1}} + \frac{W_2}{T_{g2}} \tag{10}$$

where W_1 and W_2 are the weight fractions, T_{g1} and T_{g2} are the glass transition temperatures of homopolymers 1 and 2.

Fig. 2 illustrates that T_g of the DFBP–BPA/TMBPA copolymers increases with the increase in TMBPA content, while the predicted results from the Fox equation are slightly lower than that of the experimental results. The deviation of T_g from the theoretical predictions in the copolymers could be resulted from the conformation difference between DFBP–BPA and DFBP–TMBPA homopolymers.

Table 1 shows the density of DFBP–BPA and DFBP–TMBPA homopolymers and DFBP–BPA/TMBPA random copolymers. Fraction free volumes, FFV are calculated from the relation:

$$\mathrm{FFV} = \frac{V - V_0}{V} \tag{11}$$

The specific volume, V, is calculated from the measured density and the occupied volume, V_0, is calculated from the correlation, $V_0 = 1.3V_w$, where V_w is the van der Waals volume reported by Bondi's group contribution method [19]. As for the copolymers, V_w is predicted by the equation: $V_w = m_1V_{w1} + m_2V_{w2}$, where m_1 and m_2 are the molar fractions and V_{w1} and V_{w2} are the van der Waals volume of homopolymers 1 and 2, respectively. The ideal specific free volume, $V_{f,mix}$, is used to estimate the difference between the real and ideal cases for copolymers: $V_{f,mix} = w_1V_{f1} + w_2V_{f2}$, where w_1 is the weight fraction, V_{fi} is the specific free volume of the homopolymer component i, and is equals to $V - V_0$.

As shown in Table 1, the fractional free volume increases with increasing TMBPA content in the copolymers. It also can be seen that the specific volumes of copolymers obtained from the density measurements are close to the ideal specific volume. This suggests that the chain packing in the copolymer is predictable and the permeability and selectivity are consistent with the rule of semi-logarithmic addition.

In order to reconfirm the conclusions from the FFV measurement, d-spacing values of DFBP–BPA, DFBP–TMBPA homopolymers and DFBP–BPA/TMBPA random copolymers are calculated from the WAXD results, as shown in Fig. 3. After copolymerization of TMBPA units into the copolymers, the d-spacing value increases from 4.9 Å to 5.5 Å. This indicates that the chain packing of copolymers is prohibited by the substitution of methyl groups. The change in d-spacing values of copolymers is in good agreement with that of FFV.

Table 2 summarizes the calculated results of chain properties for the DFBP–BPA/TMBPA random copolymers system. Simulated properties, which are consistent with the above experimental results, show that copolyimides consisting of a higher fraction of DFBP–TMBPA generally have a higher mean squared end-to-end distance, mean squared radius of gyration, persistence length, and molar stiffness. Clearly, the four methyl substitutions on the phenyl ring in DFBP–TMBPA units prevent the chain packing, leading to an increase in mean squared radius of gyration, which implies that more free volume could be formed between the polymer chains [20]. At the same time, the bulky side groups also hinder the phenyl ring rotation and result in an increase in rigidity of the backbone, which is

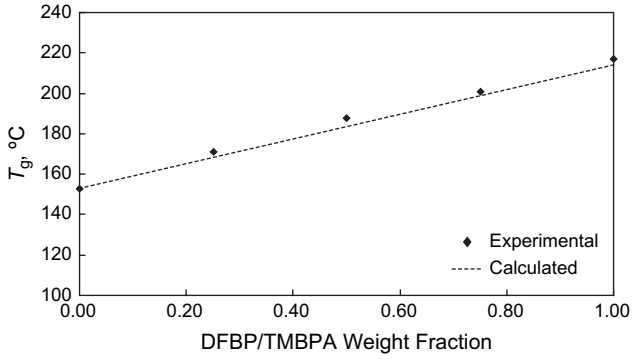

Fig. 2. Comparison of T_gs obtained from DSC experiments and calculated from the Fox equation.

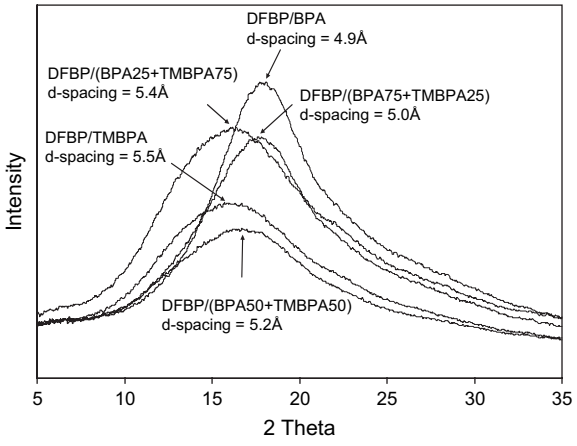

Fig. 3. d-Spacing measurement by WAXD test.

Table 2
The properties of copolymer chains (50 repeated units) at the temperature of 35 °C simulated by RMMC, Cerius2 molecular simulation software

Polymer ID	Mean squared end-to-end distance, $\langle r^2\rangle$, (Å^2)	Mean squared radius of gyration, $\langle s^2\rangle$, (Å^2)	Ratio $\langle r^2\rangle/\langle s^2\rangle$	Persistence length (mean projection on all bonds) (Å)	K_stiff ($g^{0.25}$ $cm^{1.5}$/$mol^{0.75}$)
DFBP–BPA	19,363 ± 1.46 e + 03	3192 ± 32	6.07	7.66 ± 0.17	196
DFBP–(BPA75 + TMBPA25)	19,924 ± 1.56 e + 03	3231 ± 32	6.12	7.73 ± 0.17	201
DFBP–(BPA50 + TMBPA50)	20,372 ± 1.79 e + 03	3340 ± 32	6.10	7.66 ± 0.18	207
DFBP–(BPA25 + TMBPA75)	21,061 ± 1.87 e + 03	34,245 ± 33	6.15	7.97 ± 0.19	214
DFBP–TMBPA	23,294 ± 2.24 e + 03	3804 ± 38	6.12	8.65 ± 0.20	233

Table 3
Gas permeability coefficients of random copolymers tested at 10 atm and 35 °C

Copolymers	Permeability (barrer)					Ideal selectivity		
	H_2	O_2	N_2	CH_4	CO_2	H_2/N_2	O_2/N_2	CO_2/CH_4
DFBP–BPA	11	1.0	0.16	0.18	3.5	69	6.1	19
DFBP–(BPA75 + TMBPA25)	17	1.5	0.27	0.30	5.6	63	5.7	19
DFBP–(BPA50 + TMBPA50)	25	2.5	0.46	0.49	8.8	54	5.4	18
DFBP–(BPA25 + TMBPA75)	36	3.7	0.70	0.75	13	51	5.2	18
DFBP–TMBPA	52	5.6	1.1	1.1	20	47	5.3	18

illuminated by the increase in mean squared end-to-end distance, persistence length, and the molar stiffness.

3.2. Gas transport properties of copolymers

Table 3 summarizes the pure gas permeabilities and ideal selectivities of DFBP–BPA/TMBPA copolymers. The testing temperature was maintained at 35 °C and the feed pressure was 10 atm. It was observed that the gas permeability coefficient increases with the addition of TMBPA content, while the permselectivity of the gas pairs such as H_2/N_2, O_2/N_2, and CO_2/CH_4 tends to decrease slightly or stay almost constant. It is also noted that the gas permeability coefficient decreases in the following order: $P(H_2) > P(CO_2) > P(O_2) > P(N_2) > P(CH_4)$, which agrees well with the increasing sequence of kinetic diameters of the gas molecules.

The permeability coefficients obtained from experiments and calculations based on Eq. (4) are presented in Fig. 4. The logarithm of permeability to hydrogen, oxygen, nitrogen, methane and carbon dioxide was found to increase linearly with increasing amount of DFBP–TMBPA volume fraction. The dashed lines were the calculated gas permeability. The logarithm of permeability to various gases was also plotted against 1/FFV as illustrated in Fig. 5. The experimental results of both plots are in good agreement with the predicted values, which indicates that chain-packing efficiency has a prominent effect on the gas permeation properties. The semi-logarithmic plot of permeability selectivity of the gas pairs CO_2/CH_4, O_2/N_2, and H_2/N_2 of the membranes vs. the volume fraction of DFBP–TMBPA content is presented in Fig. 6. The dashed lines are the ideal selectivities calculated using Eq. (12), which is as follows:

$$\ln\left(\frac{P_A}{P_B}\right) = \phi_1 \ln\left(\frac{P_A}{P_B}\right)_1 + \phi_2 \ln\left(\frac{P_A}{P_B}\right)_2 \quad (12)$$

where P_A and P_B are the permeability coefficient of homopolymers A and B, respectively. ϕ is the volume fraction and subscripts 1 and 2 refer to the two homopolymers. The

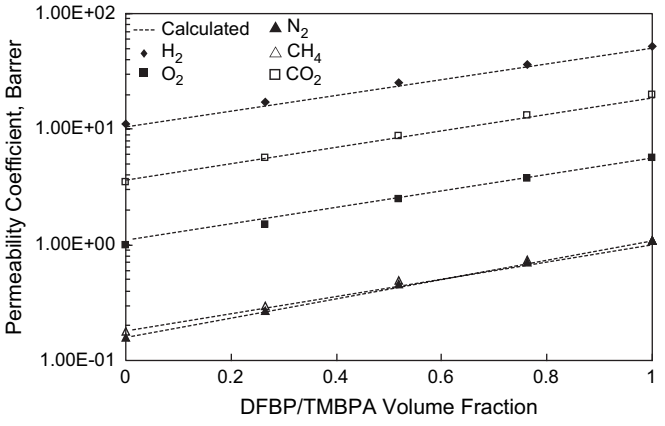

Fig. 4. Relationship between permeability coefficient vs. DFBP–TMBPA content.

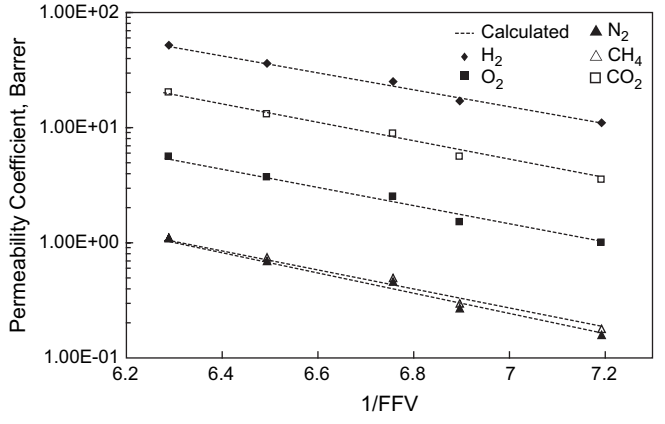

Fig. 5. Relationship between permeability coefficient vs. 1/FFV.

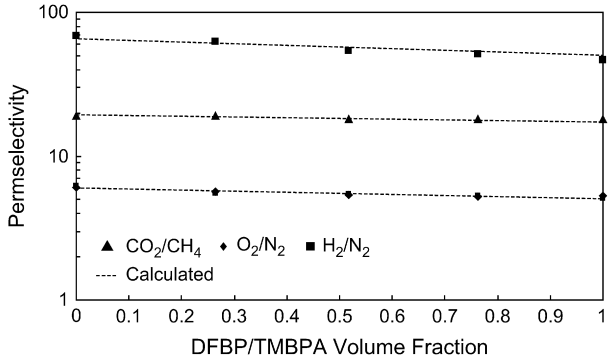

Fig. 6. Relationship between permselectivity vs. DFBP–TMBPA content.

prediction of selectivity, based on Eq. (12), is in good accordance with the experimental values.

Table 4 summarizes the apparent diffusion coefficients calculated from the time lag method with the aid of Eq. (5) and diffusivity selectivity of O_2/N_2 and CO_2/CH_4. The diffusivity coefficients of all gases increase with increasing TMBPA content can be explained by an increase in fractional free volume which leads to a looser packing of segment. The apparent solubility coefficient S_{app} calculated from Eq. (6) and solubility selectivity of O_2/N_2 and CO_2/CH_4 are summarized in Table 5. Solubility coefficient of the PAEKs follows the trend: $S(CO_2) > S(CH_4) > S(O_2) > S(N_2)$. From Table 5, it can be seen that the solubility coefficient also increases with increasing TMBPA content which is similar to the trend in the case of the diffusivity coefficient as discussed above. The high solubility of CO_2 as compared to other gases may be due to the high condensability of CO_2 molecules in the polymer matrix which can be deduced from the critical temperature [9].

Fig. 7 illustrates the relationship between gas permeability and selectivity for H_2/N_2, O_2/N_2 and CO_2/CH_4. It is obvious that the gas separation performance of all gas pairs have improved by increasing the TMBPA content in copolymers, since the separation point is approaching the tradeoff line. It is well known that the gas diffusion coefficients in the polymer matrix are determined by the activation energy and length of the penetrant jump. This activation energy is related to the polymer segmental motions and the kinetic diameter of the penetrants. In this regard, the most potential method for the development of higher performance polymeric membranes for gas separation is to increase the interchain spacing. This process increases the polymer chain stiffness and gas permeability while maintaining selectivity. This work and the results of tetramethyl substituted polycarbonate [21] show that the four methyl groups give both inhibited motion around the ether or carbonate linkage, and inhibited packing due to restriction of facile nesting conformation of the phenyl rings. Although the size of methyl groups is not big, the gas diffusion is still governed by thermally stimulated polymer segmental motions. Therefore, the methyl substitution onto the main backboned of polymer is an efficient way to improve the gas separation performance of polymeric materials.

Judging by the angle between the upper bound line and the tendency line of copolymers with increasing TMBPA content, CO_2/CH_4 and H_2/N_2 pairs show faster trend in gas separation improvement. The possible reason is that the increase in polymer interchain spacing induced by the substitution of methyl groups opens a channel for small gases, such as H_2 and CO_2, passing through with faster transport rates, but for big size gases, such as O_2, N_2 and CH_4, their gas transport is still controlled by the polymer chain thermal motion.

4. Conclusions

A series of homo/random copolymers of 4,4′-difluorobenzophenone (DFBP)–2,2-bis(4-hydroxy-phenyl)propane (BPA)/2,2-bis(4-hydroxy-3,5-dimethyl-phenyl)propane (TMBPA) in varying diol ratios were synthesized and their physical and gas

Table 4
Diffusivity coefficient and diffusivity selectivity of random copolymers tested at 10 atm and 35 °C

Copolymers	Diffusivity coefficient (10^{-8} cm^2/s)				Diffusivity selectivity	
	O_2	N_2	CH_4	CO_2	O_2/N_2	CO_2/CH_4
DFBP–BPA	3.41	0.92	0.27	1.77	3.71	6.56
DFBP–(BPA75 + TMBPA25)	4.16	1.15	0.33	2.44	3.62	7.39
DFBP–(BPA50 + TMBPA50)	5.38	1.42	0.45	3.05	3.79	6.78
DFBP–(BPA25 + TMBPA75)	6.51	1.83	0.54	4.02	3.56	7.44
DFBP–TMBPA	8.88	2.43	0.72	4.78	3.65	6.64

Table 5
Solubility coefficient and solubility selectivity of random copolymers tested at 10 atm (2 atm for CO_2) and 35 °C

Copolymers	Solubility coefficient (10^{-3} cm^3 (STP)/cm^3 cmHg)				Solubility selectivity	
	O_2	N_2	CH_4	CO_2	O_2/N_2	CO_2/CH_4
DFBP–BPA	2.83	1.78	6.53	22.11	1.59	3.39
DFBP–(BPA75 + TMBPA25)	3.66	2.35	8.76	25.96	1.56	2.96
DFBP–(BPA50 + TMBPA50)	4.59	3.18	11.15	31.18	1.44	2.80
DFBP–(BPA25 + TMBPA75)	5.76	3.77	13.73	34.70	1.53	2.53
DFBP–TMBPA	6.25	4.32	15.04	36.60	1.45	2.43

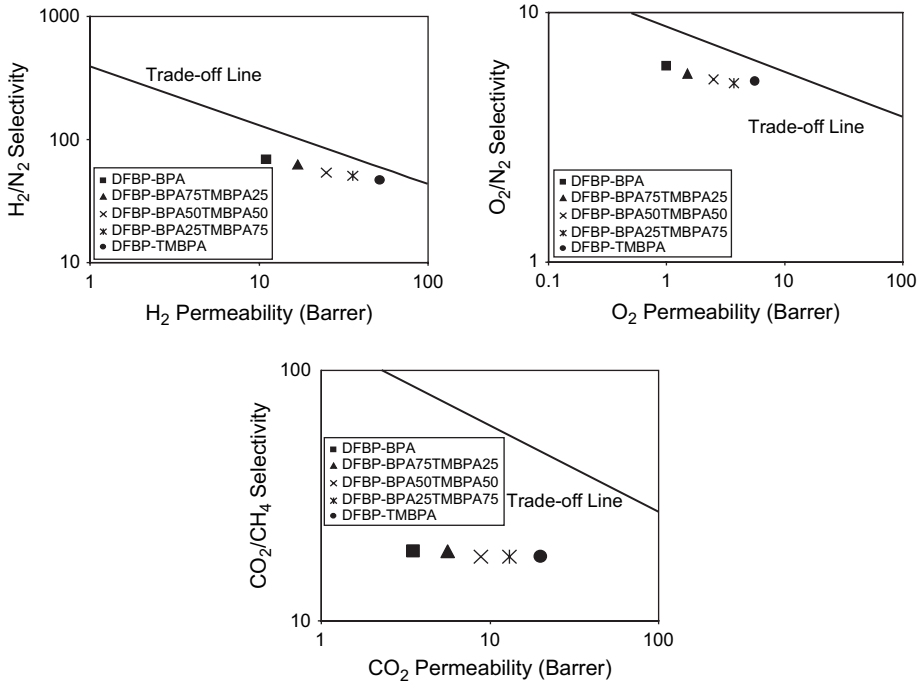

Fig. 7. Gas separation performance of PAEK copolymers.

permeation properties were studied. It was found that the incorporation of TMBPA increases the permeability, diffusivity and solubility coefficient while maintaining the permselectivity. The gas permeability was estimated by using the group contributions and the fractional free volume methods which exhibits a good agreement with experimental results.

Acknowledgements

The authors would like to thank Mitsui Chemicals, Inc. and National University of Singapore (NUS) for funding this research with the grant number of R-279-000-186-592.

References

[1] Stern SA. Polymers for gas separations: the next decade. J Membr Sci 1994;94:1.
[2] Matsuura T. Synthetic membranes and membrane separation processes. Boca Raton: CRC Press; 1994.
[3] Koros WJ, Fleming GK. Membrane-based gas separation. J Membr Sci 1993;83:1.
[4] Robeson LM. Correlation of separation factor versus permeability for polymeric membranes. J Membr Sci 1991;62:165.
[5] Freeman BD. Basis of permeability/selectivity tradeoff relations in polymeric gas separation membranes. Macromolecules 1999;32:375.
[6] Ho WSW, Sirkar KK, editors. Membrane handbook. New York: Van Nostrand Reinhold; 1992.
[7] Paul DR, Yampol'skii YP. Polymeric gas separation membranes. CRC Press; 1994.
[8] Koros WJ, Coleman MR, Walker DRB. Controlled permeability polymer membranes. Annu Rev Mater Sci 1992;22:47.
[9] Liu SL, Wang R, Chung TS, Chng ML, Liu Y, Vora RH. Effect of diamine composition on the gas transport properties in 6FDA-durene/3,3′-diaminodiphenyl sulfone copolyimides. J Membr Sci 2002;202:165.
[10] Chung TS, Lin WH, Vora RH. Gas transport properties of 6FDA-durene/1,3-phenylenediamine (*m*PDA) copolyimides. J Appl Polym Sci 2001;81:3552.
[11] Liu SL, Wang R, Liu Y, Chng ML, Chung TS. The physical and gas separation properties of 6FDA-durene/2,6-diaminotoluene copolyimides. Polymer 2001;42:8847.
[12] Lin WH, Vora RH, Chung TS. Gas transport properties of 6FDA-durene/1,4-phenylenediamine (*p*PDA) copolyimides. J Polym Sci Polym Phys 2000;38:2703.
[13] Chiou JS, Paul DR. Gas permeation in miscible homopolymer–copolymer blends II. Tetramethyl bisphenol-A polycarbonate, a styrene/acrylonitrile copolymer. J Appl Polym Sci 1987;34:1503.
[14] Kumazawa H, Wang JS, Fukuda T, Sada E. Permeation of carbon dioxide in glassy poly(ether imide) and poly(ether ether ketone) membranes. J Membr Sci 1994;93:53.
[15] Handa YP, Roovers J, Moulinie P. Gas transport properties of substituted PEEKs*. J Polym Sci Part B Polym Phys 1997;35:2355.
[16] Wang F, Chen TL, Xu JP, Liu TX, Jiang HY, Qi YH, et al. Synthesis and characterization of poly(arylene ether ketone) (co)polymers containing sulfonate groups. Polymer 2006;47:4148.
[17] Park JY, Paul DR. Correlation and prediction of gas permeability in glassy polymer membrane materials via a modified free volume based group contribution method. J Membr Sci 1997;125:23.
[18] Fox TG. Bull Am Phys Soc 1956;1:123.
[19] Bondi A. van der Waals volume and radii. J Chem Phys 1964;68:441.
[20] Tung KL, Lu KT. Effect of tacticity of PMMA on gas transport through membranes: MD and MC simulation studies. J Membr Sci 2006;272:37.
[21] Muguganandam N, Paul DR. Evaluation of substituted polycarbonated and a blend with polystyrene as gas separation membranes. J Membr Sci 1987;34:185.